

Electrical conductivity of xenon under supercritical conditions

V. B. Mintsev and V. E. Fortov

Institute of Chemical Physics, USSR Academy of Sciences

(Submitted 21 June 1979)

Pis'ma Zh. Eksp. Teor. Fiz. 30, No. 7, 401–404 (5 October 1979)

The electrical conductivity of xenon in the supercritical region, which, in terms of density, lies between the gaseous plasma and the solid state, was measured at high pressures and temperatures. The gas model can be used to describe the electrophysical properties of a medium under experimental conditions.

PACS numbers: 72.80.Cw, 51.50. + v

At present, the electronic properties of disordered systems are well known for random distribution of weakly interacting particles for which the gaseous plasma model is applicable, and for condensed media for which a large number of experiments

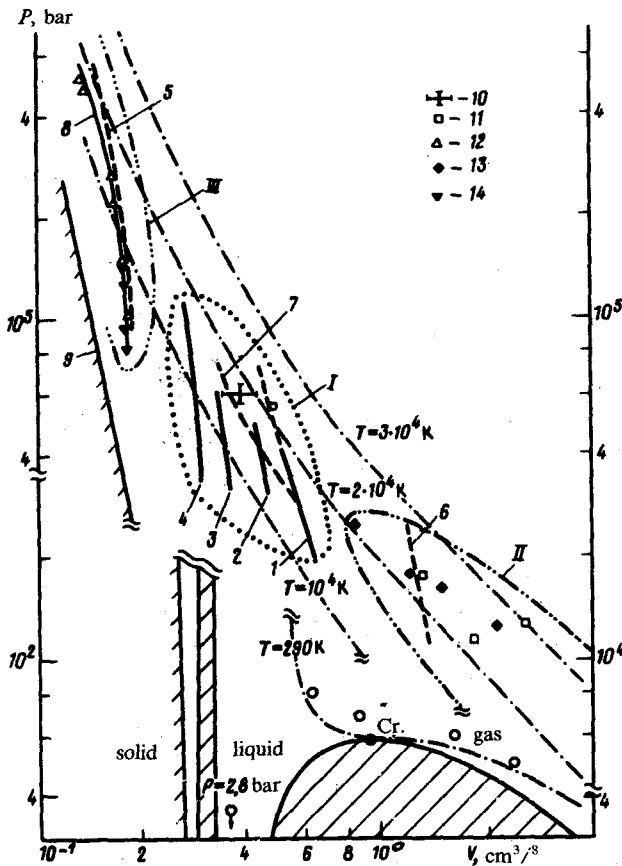


FIG. 1. Phase diagram of xenon. Calculated shock adiabats: 1— $P_0 = 50$ bar, 2— $P_0 = 60$ bar, 3— $P_0 = 70$ bar, 4— $P_0 = 80$ bar, 5— $P_0 = 2.8$ bar, $T_0 = 165$ K, 6— $P_0 = 20$ bar, 7—secondary compression shock adiabat, 8—calculations,¹⁴ 9—isootherm, $T = 0$ K. Thermodynamic measurement data: 10—"reflection" method, 11—Ref. 5, 12—Ref. 4; measurement of electrical conductivity: 13—Ref. 2, 14—Ref. 4.

with liquid metals and doped semiconductors is adequately described by the pseudopotential models. Of particular interest is the intermediate case of the near-critical and supercritical densities in which a strong interaction between the particles renders useless the kinetic equations, and the development of semi-empirical models is hindered by almost complete absence of experimental data.⁽¹⁾

In this work we measured the static electrical conductivity of xenon under highly supercritical conditions $\rho \sim 1-4 \text{ g/cm}^3$ ($\rho_{cr} = 1.1 \text{ g/cm}^3$) at high pressures ($P \sim 20 - 110 \text{ kbar}$) and temperatures [$T \sim (1-2) \times 10^4 \text{ K}$] (Fig. 1); a broad spectrum of strong interparticle interaction, including the neutral and charged particles, was obtained. The investigated region of parameters I (Fig. 1) extends from the states with reduced density II, where the electrophysical and thermodynamic properties of a material are described by the plasma models,^(2,3) to the region III of solid-state densities⁽⁴⁾ produced by shock compression of liquid xenon, in which the shock compressibility of the system is described by the band theory of solids, and the electrical conductivity is in agreement with the semiconductor models.

The generation of selected states (region I) was accomplished by dynamic compression and heating of xenon at near-critical parameters $P_0 \sim 50-80 \text{ bar}$, $T_0 \sim 298 \text{ K}$, $\rho_0 \sim 0.4-1.6 \text{ g/cm}^3$ (denoted by circles in Fig. 1). The experiments were performed in an explosive device.⁽²⁾ The static electrical conductivity was measured by using a four-probe method. The shock wave velocity was measured in each experiment by using a base electrical contact method (Fig. 2). These measurements showed a substantial attenuation of the shock wave, which indicates that the parameters of the shock-compressed material are nonuniform (up to 20%); this was taken into account in the analysis of all the data obtained experimentally.

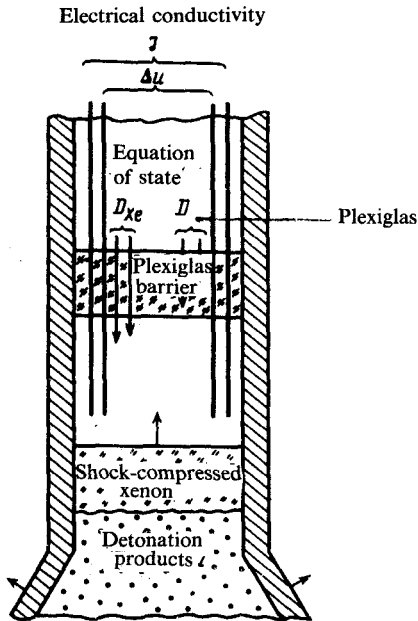


FIG. 2. Experimental setup.

To verify the thermodynamic model used in the subsequent analysis, we performed a series of experiments to refine the caloric equation of state for xenon by using the "reflection" method (Fig. 2). A plane Plexiglas barrier was placed ~ 7 cm from the explosive charge. The velocity of the shock wave in xenon was recorded as it approached the barrier, and the velocity of the shock wave in the Plexiglas barrier was measured. This enabled us to determine the pressure ($\pm 5\%$), the density, and the enthalpy ($\pm 15\%$) of xenon after it was compressed twice in the direct and reflected shock waves (point 10 in Fig. 1). To describe the thermodynamic properties of xenon, we used a "chemical" model in which the Coulomb interaction of charges was described by a modified Debye approximation,⁽³⁾ and the repulsion of atoms and ions at small distances was reconstructed by the virial expansion in the framework of the Lenard-Jones potential, i.e., the second and third virial coefficients were used. It can be seen (dashed line in Fig. 1) that this model describes satisfactorily the results of single⁽⁵⁾ and double compression of gaseous xenon and reproduces the results obtained in the shock compression of a liquid⁽⁴⁾ to within a 10% accuracy.

The obtained experimental values of the electrical conductivity of xenon are in the range of 10 to 250 mho/cm. On the whole, there is a reasonable agreement with the earlier measurements in the region II⁽²⁾ and with the results of investigation of the

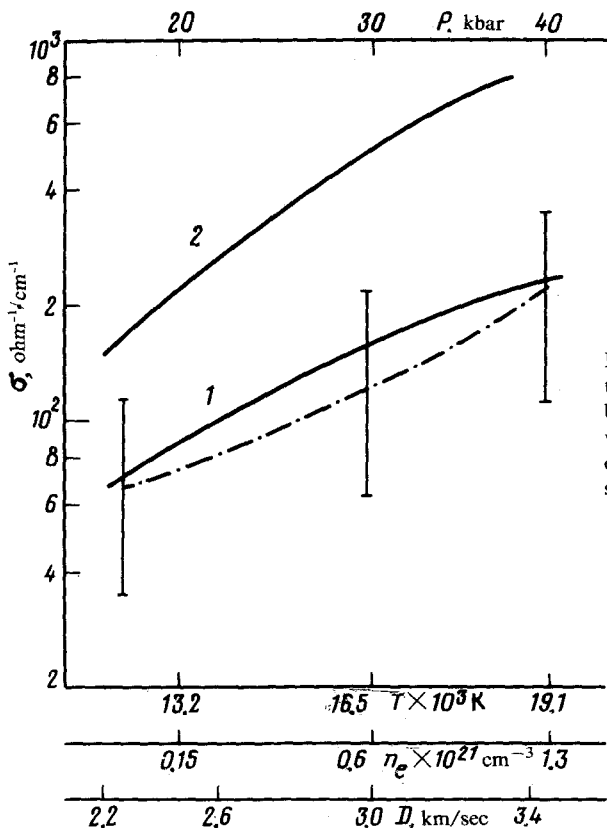


FIG. 3. Electrical conductivity for the xenon shock adiabat at $P_0 = 50$ bar. The abscissa shows calculated values of pressure, temperature and electron density at the front of the shock discontinuity.

solid-state densities.⁽⁴⁾ On going from region III to region II the electrical conductivity increases monotonically from $\sigma \sim 1$ mho/cm at $T \sim 7 \times 10^3$ K in the condensed xenon to $\sigma \sim 500$ mho/cm in the nonideal plasma ($T \sim 2.5 \times 10^4$ K). Figure 3 shows the results of measurements of the electrical conductivity at $P_0 = 50$ bar (dash-dot line), as a function of the velocity of the shock wave. The following interpolation expression obtained in the τ approximation was used to estimate the conductivity under the experimental conditions:

$$\sigma = \frac{4e^2}{3\sqrt{\pi} m_e} \frac{\bar{Z}}{\bar{Z}} \int_0^{\infty} \frac{x^{3/2} \exp(-x) dx}{v_{ea}(x) + \gamma v_{ei}(x)},$$

where \bar{Z} is the activity which is related, in terms of the radial Debye approximation, to the electron concentration n_e by the relation $\bar{Z} = n_e / (1 + \bar{\gamma}/2)$.⁽³⁾ The electron-ion collision frequency v_{ei} was calculated according to the modified Zai'man theory.⁽⁶⁾ The calculations (curve 1) are in satisfactory agreement with the experiment. Figure 3 also shows the calculation with $\bar{Z} = n_e$ (curve 2), which corresponds to the generally accepted calculations.⁽⁶⁾ Thus, the obtained data for the electrical conductivity can be satisfactorily described by using the gas plasma model.

In conclusion, the authors thank V.K. Gryaznov for his help with the thermodynamic calculations and G.A. Pavlov and A.N. Dremin for useful discussions.

¹V. A. Alekseev, N. A. Andreev, and V. Ya. Prokhorenko, *Usp. Fiz. Nauk* **106**, 393 (1972) [*Sov. Phys. Usp.* **15**, 139 (1972)].

²Yu. V. Ivanov, V. B. Mintsev, V. Ye. Fortov, and A. N. Dremin, *Zh. Eksp. Teor. Fiz.* **71**, 216 (1976) [*Sov. Phys. JETP* **44**, 112 (1976)].

³V. K. Gryaznov, I. L. Iosilevskii, and V. Ye. Fortov, *Prikl. Mekh. Tekh. Fiz.* No. 3, 73 (1973).

⁴R. N. Keeler, M. van Thiel, and B. J. Adler, *Physica* **31**, 1437 (1965). R. Keeler, *Sb. Fizika vysokikh plotuostei energii* (Coll. High-density Energy Physics), P. Calderola and G. Knopfell, Eds., (Russian Translation) M., Mir, 1974, p. 120.

⁵V. Ye. Fortov, A. A. Leont'ev, V. K. Gryaznov, and A. N. Dremin, *Zh. Eksp. Teor. Fiz.* **71**, 225 (1976) [*Sov. Phys. JETP* **44**, 116 (1976)].

⁶V. K. Gryaznov, Yu. V. Ivanov, A. N. Starostin, and V. Ye. Fortov, *Teplofiz. Vys. Temp.* **14**, 3 (1976).